

Collisional and radiative excitation transfers in Kr-Xe mixtures: Quenching of Kr

Jerry D. Cook and P. K. Lechner*

Department of Physics and Astronomy, Eastern Kentucky University, Richmond, Kentucky 40475

(Received 6 February 1984; revised manuscript received 7 August 1984)

A detailed study of electronic energy transfers in Kr-Xe mixtures has been made using a 250-keV electron accelerator to excite Kr-Xe mixtures over a wide range of Kr-host-gas pressure and Xe-impurity concentrations. Kr pressure ranged from 25 to 900 Torr with Xe concentrations varying from 0.1% to 10% of Kr partial pressure. Emission spectra taken in the vacuum-ultraviolet (vuv) region indicate that energy is transferred efficiently from Kr to Xe, with radiation from the $\text{Xe}(^3P_1)$ state becoming greatly enhanced as the Xe-impurity concentration is increased. Emission spectra from the vuv also show that the $\text{Xe}(^1P_1)$ state is populated by absorption of photons emitted from the Kr_2^* first continuum. Two-body quenching rates with Xe ground-state atoms have been found for the $\text{Kr}(^1P_1)$ [$k_q(1165 \text{ \AA})=1.2 \times 10^5 \text{ sec}^{-1}/\text{Torr}$] and for the $\text{Kr}(^3P_1)$ [$k_q(1236 \text{ \AA})=9.5 \times 10^5 \text{ sec}^{-1}/\text{Torr}$] resonance states. Time-resolved measurements have also been made on the Kr_2^* first and second continua. These measurements show the $\text{Kr}(^3P_1)$ state is the atomic precursor of the Kr_2^* first continuum. The results obtained in the Kr_2^* second continuum are rate limited by the decay of $\text{Kr}(^3P_1)$ at large Xe-impurity concentrations.

INTRODUCTION

Measurements of the time dependence of the emissions from noble gases excited with energetic electrons or protons have provided much new information about the excitation and relaxation of atomic and molecular species. The ability to rapidly inject energy into gases over wide pressure ranges makes it possible to determine collision coefficients and molecular lifetimes that would be difficult to obtain from other types of experiments or from theory. In the past, fast electron beams have been used by this group in spectroscopic studies of vacuum ultraviolet (vuv) emissions from Ar,¹ Kr,² Ne,³ Xe,⁴ and He-Ne mixtures.⁵ This work is an extension of that study.

Detailed knowledge of atomic collision rates and of excimer formation and decay is essential for an understanding of the mechanisms which lead to stimulated emission in high-pressure noble gases.⁶ In particular, time-resolved information obtained from spectroscopic studies of noble gases provides two- and three-body collision rates for excited atomic states. In general, two-body rates correspond to atom-atom energy transfers whereas three-body rates imply excimer formation processes. Information about the rate coefficients is invaluable in determining energy pathways in the noble gases.

We have made a detailed study of electronic energy transfers in Kr-Xe gas mixtures. This study is concentrated to a large extent on the vuv region where the lower-lying resonance states of Kr and Xe radiate. Electronic energy transfers in Kr-Xe gas mixtures were investigated over a wide pressure range. Kr-host-gas pressure was varied from 25 to 900 Torr with Xe-impurity concentrations ranging from 0.1% to 10%. Measurements were made over this wide range of host-gas pressure and impurity concentration to determine reaction rates in Kr-Xe mixtures and to make a meaningful comparison with results which had previously been obtained for pure Kr and

Xe. This has provided an important test for the experimental method and data analysis used in this work. This paper deals with vuv emissions in Kr and discusses energy transfers from Kr to Xe. A second work is planned that will present a model for electronic energy transfers in pure Kr. A third paper will present results obtained from vuv emissions from Xe and a study of Kr-Xe emissions in the visible and near-infrared regions.

Two-body quenching rates by Xe ground-state atoms were determined for the $\text{Kr}(^1P_1)$ and $\text{Kr}(^3P_1)$ resonance states. In addition, extrapolation to zero Xe impurity gave good agreement with the pressure-dependent lifetimes reported for these states² in a study of pure Kr. Emissions from the Kr_2^* continua were investigated at the wavelength region of the Kr_2^* first continuum from 1250 to 1300 Å and at 1430 Å which lies in the Kr_2^* second continuum wavelength region.

Figure 1 shows an energy-level diagram of Kr and Xe. Specifically, this diagram shows all Kr and Xe levels that lie lower in the energy spectrum than the $\text{Kr}(^1P_1)$ resonance state. The Kr levels are denoted by the *L-S* coupling scheme to facilitate comparison with previous studies. Similarly, the lowest excited states of Xe are given in both *L-S* and *j-l* coupling whereas the more appropriate *j-l* coupling is used for the higher-lying levels. All energy levels are taken from Moore.⁷

It is evident that sufficient overlap of Kr and Xe levels exists to merit investigation. Inspection of Fig. 1 shows that all four of the lower-lying states of Kr have accidental near-resonances with excited states of Xe. Additionally, the two Kr continua shown in Fig. 1 energetically overlap a number of Xe excited states. We have, therefore, investigated the possibilities of both atom-atom and molecule-atom energy transfers between the two gases. The manifold of Xe levels shown also indicates that energy transfers out of the vuv region might be expected.

Quenching rates for the Kr and Xe resonance states

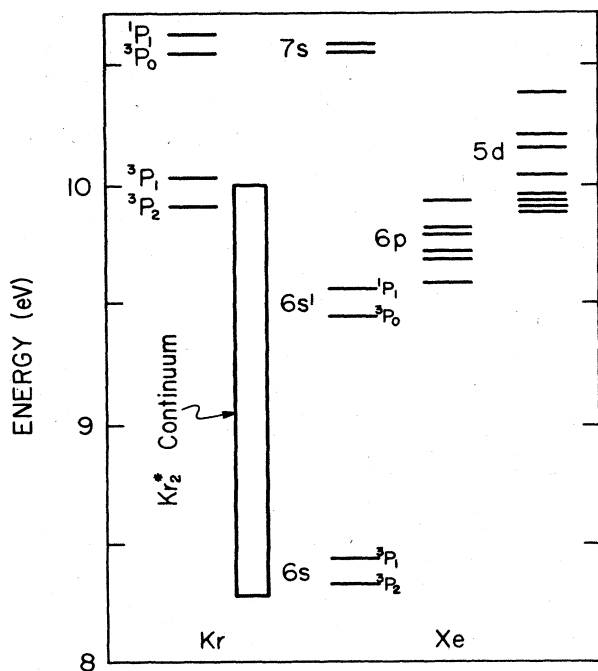


FIG. 1. Energy-level diagram for Kr and Xe showing the lowest excited states of Kr, the Kr_2^* continuum, and nearby Xe levels.

have not previously been measured in Kr-Xe mixtures. Time-dependent measurements appear to be limited to measurements made in the Kr_2^* second continuum and the Xe_2^* second continuum by Salamero *et al.*⁸ and a quenching study of the $\text{Kr}(^3P_2)$ metastable population by Velazco *et al.*⁹ Emission spectra presented by Gedanken *et al.*,¹⁰ Cheshnovsky *et al.*,¹¹ and by Salamero *et al.*⁸ in

the vuv region show considerable enhancement of the radiation from the $\text{Xe}(^3P_1)$ resonance state and the Xe_2^* continua in Kr-Xe mixtures.

While no previous time-resolved studies have been made for the $\text{Kr}(^1,^3P_1)$ resonant states in Kr-Xe mixtures, there are investigations² for pure Kr. A detailed comparison with the results obtained in that study is given in this paper.

Interest in new efficient laser candidates should make this work especially relevant. It provides new information on energy pathways in Kr-Xe mixtures. The development of the rare-gas-monohalide lasers should further heighten interest in this work and similar time-resolved studies.

EXPERIMENTAL METHOD

The experimental equipment and techniques used in this experiment are described in the literature (see, for example, Thonnard and Hurst,¹ and Leichner *et al.*⁴). The following discussion is included for completeness.

A schematic diagram of the apparatus is shown in Fig. 2. The gas handling system, including the emission cell and valves, is made of stainless steel. Ultrahigh-purity pressure reducers are used on the high-pressure gas cylinders. The entire system is evacuated to less than 10^{-7} Torr for at least 24 hours prior to taking data. Commercially available Kr and Xe gas (research grade, 99.9995% purity) is mixed turbulently in a small mixing tank of volume 1.25 l. Pressure in the tank and the emission cell is monitored with a capacitance manometer whose sensing head has a range from 1 to 1200 Torr. The manometer has a sensitivity of 0.005% of readout and is equipped with a five-place digital pressure indicator. When taking data, gas is slowly flowed through the emission cell at a rate of about 1 ml per min.

The incident beam of 250-keV electrons produces a nar-

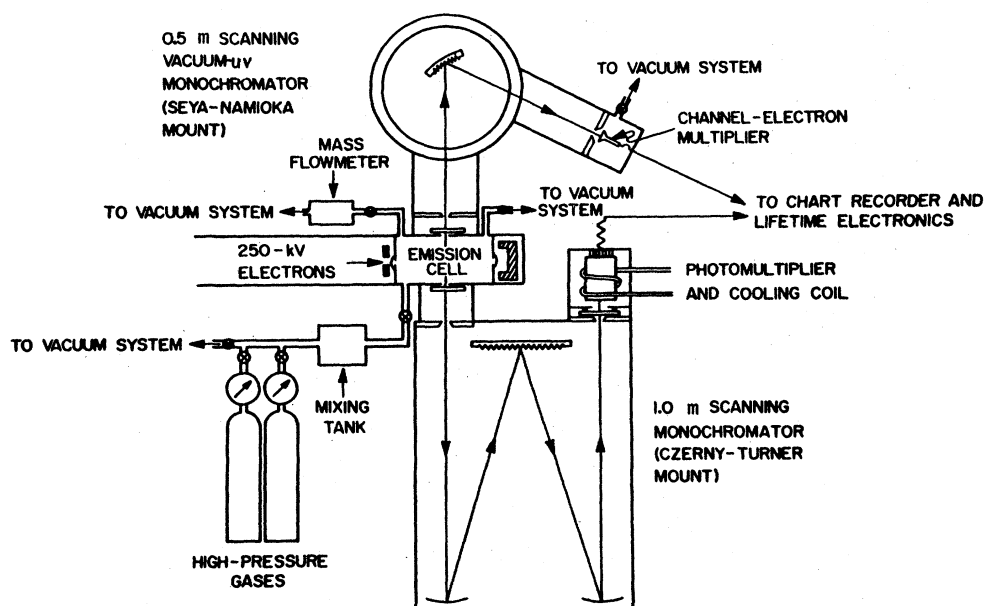


FIG. 2. Schematic diagram showing the experimental arrangement used in this experiment.

row pencil of excited species along the axis of the cylindrical emission cell which is sealed on both ends with thin metal foils. The cell has a radius of 1 cm and a length of 3.5 cm. Electron pulse widths are variable from 40 to 400 nsec with repetition rates ranging from 10 to 125 kHz. Pulse widths used in this experiment were less than 100 nsec with average currents of less than 5 nA. Photons emitted by the excited gas enter either of two scanning monochromators through LiF windows. The vuv monochromator is equipped with a channel-electron multiplier (CEM) for single-photon counting. The 1-m instrument utilizes an 11-dynode GaAs photomultiplier for wavelengths from about 300 to 900 nm. The spontaneous emissions from electron-beam excited gas mixtures can therefore be monitored under identical excitation conditions over wavelengths extending from the vuv to the infrared. Time-resolved measurements are made using a time-of-flight technique and commercially available electronic components. Reference 1 describes this procedure in great detail.

The estimated experimental error in the quenching rates is 5% because these are based on average values. The error in other collisional decay rates is estimated at 10%.

EXPERIMENTAL RESULTS

Time-resolved spectra of the vuv emissions from Kr-Xe mixtures are shown in Figs. 3–5. These spectra are not corrected for the wavelength-dependent efficiency of the CEM which decreases exponentially at longer wavelengths. For a more realistic picture of continua emissions in the 1400–1600-Å region see the spectra presented by Salamero *et al.*⁸ Although the time-unresolved spectra presented here are largely self-explanatory, we discuss some of the prominent features for later reference.

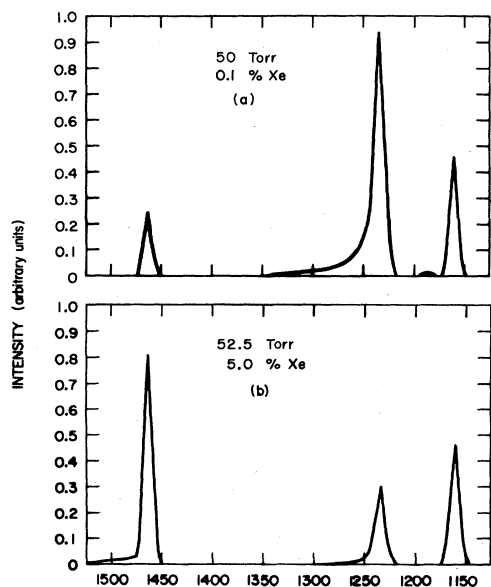


FIG. 3. Low-pressure emission spectra of Kr-Xe gas mixtures in the vuv region. Krypton pressure is 50 Torr with Xe impurities of 0.1% and 5% of Kr partial pressure added.

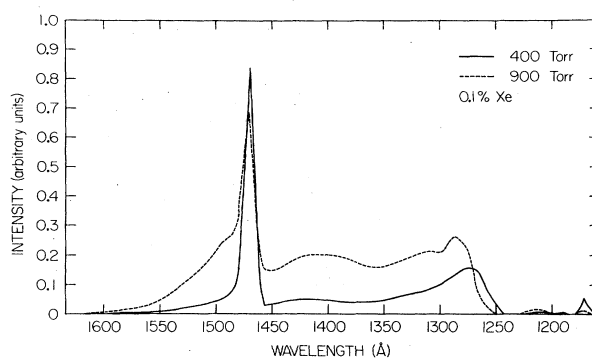


FIG. 4. High-pressure emission spectra with Xe impurity of 0.1% of Kr partial pressure added to Kr partial pressures of 400 and 900 Torr.

Figure 3 shows typical spectra for low Kr-host-gas pressures (less than 100 Torr). These spectra consist almost entirely of the well-known emissions corresponding to transitions of the two Kr resonant states: $\text{Kr}(^1P_1)$ to $\text{Kr}(^1S_0)$ at 1165 Å and $\text{Kr}(^3P_1)$ to $\text{Kr}(^1S_0)$ at 1236 Å, and the $\text{Xe}(^3P_1)$ to $\text{Xe}(^1S_0)$ transition at 1470 Å. As Xe impurity concentration is increased, Fig. 3 shows that Kr excitation is transferred to Xe because the Xe radiation intensity at 1470 Å is strongly enhanced while the Kr emissions at 1236 Å are severely quenched. At low Kr-host-gas pressures formation of Kr_2^* molecules is considered to be unimportant. This means that the $\text{Kr}(^3P_1)$ level and the $\text{Xe}(^3P_1)$ level are energetically linked through atomic pathways. Comparison with emission spectra for pure Xe under identical excitation conditions has shown that at the low Xe-impurity concentration shown in Fig. 3 direct excitation of Xe by the electron beam is negligible.

Figures 4 and 5 show typical spectra for high Kr-host-gas pressures with different Xe-impurity concentrations. These spectra exhibit well-known emissions from Kr_2^* molecular states² in the region 1240–1470 Å, resonance radiation from $\text{Xe}(^3P_1)$ to $\text{Xe}(^1S_0)$ at 1470 Å, and the emergence of Xe molecular radiation on the long-wavelength side of the $\text{Xe}(^3P_1)$ emissions. The emissions from Xe will be discussed in a later work. However, we

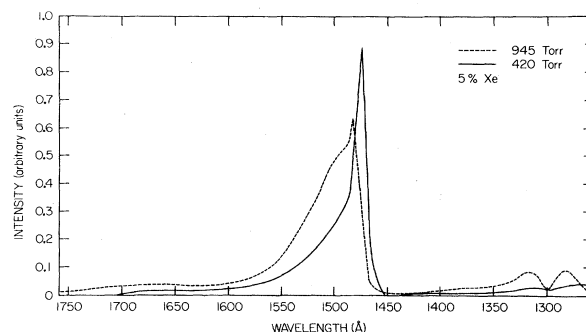


FIG. 5. High-pressure emission spectra with Xe impurity of 5% of Kr partial pressure added to Kr partial pressures of 400 and 900 Torr.

note that Cheshnovsky *et al.*¹¹ have assigned these emissions to represent radiation from KrXe^* molecules. In our quenching study of Kr, we are particularly interested in the following features of the high-pressure spectra: the severe quenching of the Kr_2^* molecular continua, the absorption line at 1296 Å, and the complete quenching of the radiation from the two Kr resonant states. Comparison with vuv emission spectra from pure Xe has shown direct excitation of Xe by the electron beam is not negligible in the 5% spectra and contributes 15–20% of total Xe emissions. Since we do not use these emission intensities in our time-resolved studies, their effects can be ignored.

The emission spectra shown indicate that there are several energy-transfer mechanisms between Kr and Xe. These processes are discussed in detail after the time-dependent results obtained in this work are presented.

To obtain quantitative information about excitation transfer in Kr-Xe mixtures, we have made time-resolved measurements for the following Kr excited species: the $\text{Kr}(^1,^3P_1)$ resonance states at 1165 and 1236 Å, respectively, the Kr_2^* first-continuum emissions in the 1260–1290-Å region, and the Kr second-continuum emissions in the 1430-Å region. Data were taken over Kr pressure and Xe-impurity concentration ranges such that a family of decay curves was obtained for each excited state. This has made it possible to interpret the vuv data with a minimum of kinetic modeling and to make comparisons with previous work on pure Kr.

The time dependence of emission intensities for all the excited species of Kr that we have studied can be fit to a sum of exponential decays of the form

$$I(t) = A_1 e^{-\gamma_1 t} + A_2 e^{-\gamma_2 t}, \quad (1)$$

where $\gamma_{1,2}$ represent the total decay constants which in general contain radiative and collisional decay terms as

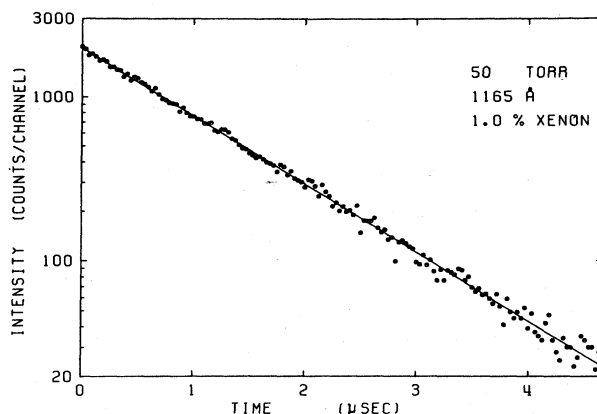


FIG. 6. Typical decay curve of the $\text{Kr}(^1P_1)$ emissions in Kr-Xe mixtures. Krypton partial pressure is 50 Torr and Xe impurity is 1% of Kr partial pressure.

shown below. Only one term of Eq. (1) was required to fit the decay of the $\text{Kr}(^1P_1)$ resonant state. The $\text{Kr}(^3P_1)$ and Kr_2^* emissions are characterized by one-exponential decays at low Xe impurities and by two-exponential decays at large Xe impurities. The results given for the $\text{Kr}(^3P_1)$ resonant state and the Kr_2^* continua are obtained from analysis of the fast-decay component of the exponential decay curves. We were unable to find any systematic pressure dependence for the slow-decay component found at higher Xe impurities and have not included it in our kinetic scheme. Therefore, γ denotes only the decay constant obtained for the fast-decay component at each wavelength. A representative time-resolved spectrum for the $\text{Kr}(^1P_1)$ resonant state is shown in Fig. 6.

We have found that the decay constants of each of these states can be predicted by an equation of the form

TABLE I. Collision coefficient for Kr as explained in the text.

Excited state	λ (Å)	Source	β (sec ⁻¹)	k_1 (sec ⁻¹ /Torr)	k_2 (sec ⁻¹ /Torr ²)	k_q (sec ⁻¹ /Torr)
$\text{Kr}(^1P_1)$	1165	This work	1.9×10^5	1.4×10^4	0.0	1.2×10^5
		Literature		1.3×10^4 ^a	0.0	
$\text{Kr}(^3P_0)$	1174	This work				
		Literature				
$\text{Kr}(^3P_1)$	1236	This work	1.7×10^5	5500	9.0	9.5×10^5
		Literature		6000 ^a	8.5 ^a	
				5600 ^b		
$\text{Kr}(^3P_2)$	1250	This work				
		Literature		75 ^c	44 ^c	5.3×10^5 ^d
Kr_2^*	1240–1300	This work		5500	9.0	9.5×10^5
		Literature		6000 ^a	8.5 ^a	
Kr_2^*	1430	This work		5800	10.0	9.5×10^5
		Literature	4×10^6 ^e			2×10^7 ^f
			3.3×10^5 ^a			

^aLeichner (Ref. 2).

^bTheineman (Ref. 11).

^cTurner (Ref. 21).

^dVelazco (Ref. 9).

^eSalamero (Ref. 20).

^fSalamero (Ref. 8).

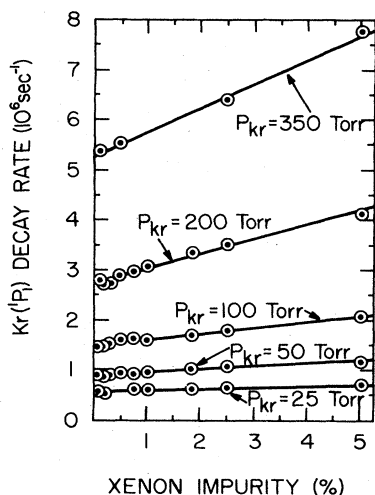


FIG. 7. $\text{Kr}(^1P_1)$ decay rate in Kr-Xe mixtures as a function of Xe impurity and Kr pressure ranging from 25 to 350 Torr. Xe impurity is plotted as a percentage of Kr partial pressure.

$$\gamma = \beta + k_1 P_{\text{Kr}} + k_2 P_{\text{Kr}}^2 + k_q P_{\text{Xe}}, \quad (2)$$

where β denotes the escape of imprisoned resonance from the emission cell, k_1 represents the two-body collision rate with Kr ground-state atoms, k_2 represents a three-body collision rate with Kr ground-state atoms, and k_q (the quenching rate) represents the two-body collision rate with Xe ground-state atoms. A complete summary of our measured values for these terms is provided by Table I, as is a list of values found in the literature. For ease in notation the decay constants are further identified by wavelength rather than spectroscopic notation. As an example to illustrate our data analysis, we present pressure-dependent results obtained for the $\text{Kr}(^1P_1)$ state at 1165 Å. All other pressure-dependent results are obtained in an identical procedure.

The results of time-resolved measurements for the $\text{Kr}(^1P_1)$ resonance level are shown in Fig. 7. The solid lines are least-squares fits to the data. In this and all following sets of data we have plotted the decay constants of the excited states as a function of Kr partial pressure and Xe impurity in percent. Consequently, the range of Xe partial pressures is different for each Kr pressure. This is reflected in the figure by different slopes. In terms of Kr

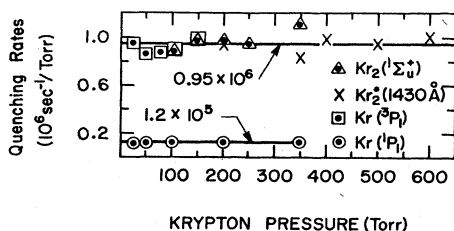


FIG. 8. Quenching rates of the Kr emissions vs Kr partial pressure.

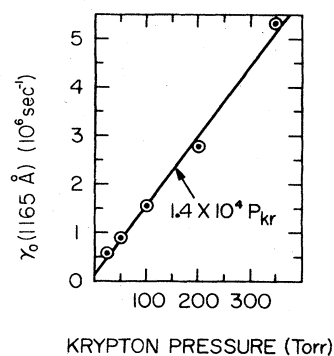


FIG. 9. Intercepts $\gamma_0(1165 \text{ \AA})$ obtained from the data in Fig. 9 vs Kr pressure. Solid line is the two-body destruction rate of $\text{Kr}(^1P_1)$ by Kr ground-state atoms.

pressure and Xe-impurity concentration in percent, Xe partial pressure is given by

$$P_{\text{Xe}} = f(\%) P_{\text{Kr}} / 100, \quad (3)$$

where $f(\%)$ denotes Xe impurity in percent, and P_{Kr} is the Kr partial pressure. The quenching rate due to Xe impurity is calculated from $\Delta\gamma/P_{\text{Xe}}$ where $\Delta\gamma$ is the variation in the decay constant corresponding to the range P_{Xe} of Xe partial pressure. Quenching rates for all excited states of Kr as a function of Kr partial pressure are summarized in Fig. 8.

The quenching rate of the $\text{Kr}(^1P_1)$ resonance state is calculated from the data in Fig. 7 as explained above, and the results are plotted in Fig. 8. For the $\text{Kr}(^1P_1)$ state the total decay constant $\gamma(1165 \text{ \AA})$ contains a radiative term, a two-body collision term for the destruction by Kr ground-state atoms, and the quenching rate k_q . Three-body destruction by Kr or Xe ground-state atoms need

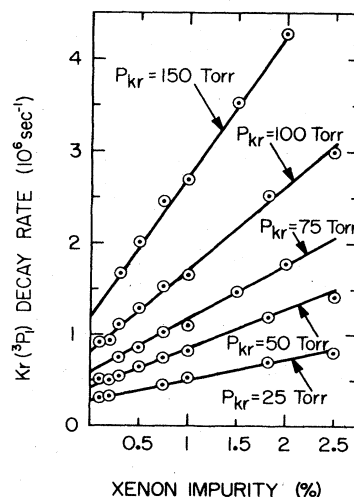


FIG. 10. $\text{Kr}(^3P_1)$ decay rate in Kr-Xe mixtures as a function of Xe impurity and Kr pressure ranging from 25 to 150 Torr. Xe impurity is plotted as a percentage of Kr partial pressure.

not be considered because all the decays are linear as a function of Kr pressure and Xe impurity. The decay rate of the 1165-Å radiation may therefore be written as

$$\gamma(1165 \text{ \AA}) = \beta(1165 \text{ \AA}) + k_1 P_{\text{Kr}} + k_q P_{\text{Xe}}. \quad (4)$$

It is useful to write this equation in the form

$$\gamma(1165 \text{ \AA}) = \gamma_0(1165 \text{ \AA}) + k_q P_{\text{Xe}}, \quad (5)$$

where

$$\gamma_0(1165 \text{ \AA}) = \beta(1165 \text{ \AA}) + k_1 P_{\text{Kr}} \quad (6)$$

so that $\gamma_0(1165 \text{ \AA})$ is independent of Xe pressure and can be obtained from the intercepts which correspond to zero impurity. The intercepts of the $\text{Kr}(^1P_1)$ decay constants are plotted in Fig. 9. A least-squares fit to these intercepts yields $\beta(1165 \text{ \AA}) = 1.9 \times 10^5 \text{ sec}^{-1}$ and $k_1 = 1.4 \times 10^4 \text{ sec}^{-1}/\text{Torr}$. A least-squares fit of the data presented in Fig. 7 yields an average of $k_q = 1.2 \times 10^5 \text{ sec}^{-1}/\text{Torr}$. k_q is constant over the entire range of Kr pressure and Xe impurity. As seen from Table I the two-body rate k_1 is in good agreement with the results of Lechner and Ericson² for pure Kr. Values of the quenching rate k_q have not been found in the literature so that comparison with previous work is not possible. However, errors in the measured quenching rates would lead to incorrect intercepts and erroneous decay rates for pure Kr. This quenching rate is interpreted to represent electronic energy transfers from $\text{Kr}(^1P_1)$ to nearby $\text{Xe}(7s)$ excited atomic states as discussed in the next section.

The results of time-resolved measurements for the $\text{Kr}(^3P_1)$ resonant state are shown in Fig. 10, time-resolved measurements for the Kr_2^* first continuum are shown in Fig. 11, and time-resolved measurements for the Kr_2^* second continuum are presented in Fig. 12. The pressure dependence obtained for these excited states is shown in Table I. The analytical procedure that we have used in

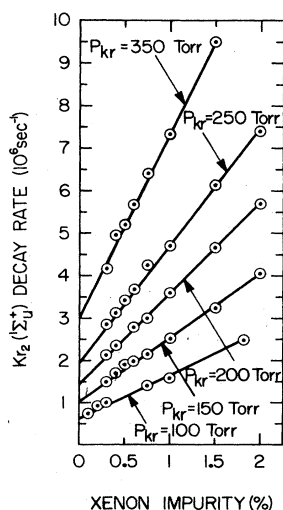


FIG. 11. $\text{Kr}_2^*(^1\Sigma_u)$ decay rate in Kr-Xe mixtures as a function of Xe impurity and Kr pressure ranging from 100 to 350 Torr. Xe impurity is plotted as a percentage of Kr partial pressure.

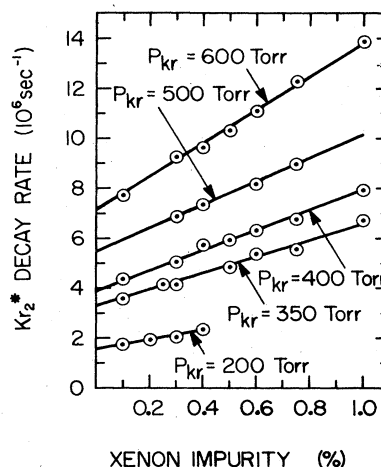


FIG. 12. Decay rates of the 1430-Å emissions in Kr-Xe mixtures. Xe impurity is plotted as a percentage of Kr partial pressure.

obtaining all results shown in Table I is identical with that explained in our analysis of emissions from the $\text{Kr}(^1P_1)$ resonant state. Figure 13 displays the intercepts obtained from Figs. 10 and 11 corresponding to zero Xe impurity. Following the notation we have adopted, $\gamma_0(1236 \text{ \AA})$ will denote the intercepts in Fig. 10 corresponding to zero Xe impurity, and $\gamma_0(1260 \text{ \AA})$ will be used to identify the intercepts from Fig. 11. To facilitate comparison of the pressure dependence of these two quantities, the linear quantities $\gamma_0(1260 \text{ \AA})/P_{\text{Kr}}$ and $[\gamma_0(1236 \text{ \AA}) - \beta(1236 \text{ \AA})]/P_{\text{Kr}}$ are displayed simultaneously. When presented in this way, the intercept of the least-squares fit to the data shown in Fig. 13 gives k_1 and the slope represents k_2 . Figure 13 also shows that our experimental values of k_1 and k_2 are the same for the $\text{Kr}(^3P_1)$ resonant state and the Kr_2^* first continuum.

The quenching rate $k_q = 9.5 \times 10^5 \text{ sec}^{-1}/\text{Torr}$ that we have measured is constant over the entire range of Kr pressure and Xe impurity that we have studied. No values of this rate have been found in the literature. How-

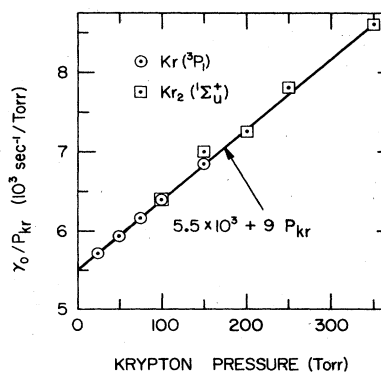


FIG. 13. Two- and three-body decay rates of $\text{Kr}(^3P_1)$ atoms obtained from the data in Figs. 12 and 13, as explained in the text.

ever, the rates $k_1 = 5500 \text{ sec}^{-1}/\text{Torr}$ and $k_2 = 9 \text{ sec}^{-1}/\text{Torr}^2$ can be compared to other works. The data obtained by Leichner and Ericson² in pure Kr (see Tables II and III, Ref. 2) indicate that k_1 is about $6000 \text{ sec}^{-1}/\text{Torr}$, and k_2 is about $8.5 \text{ sec}^{-1}/\text{Torr}^2$. Thieman¹² found a value of $5600 \text{ sec}^{-1}/\text{Torr}$ for k_1 in a study of Ar-Kr mixtures. The analysis of Kr_2^* second-continuum emissions is summarized in Table I.

KINETIC ANALYSIS

Our spectroscopic study has allowed us to identify the following energy transfers from Kr to Xe: (i) transfers of energy from the $\text{Kr}(^1P_1)$ and the $\text{Kr}(^3P_1)$ resonant states to excited states of Xe in two-body collisions with Xe ground-state atoms, (ii) absorption of photons emitted by the Kr_2^* first continuum by the $\text{Xe}(^1P_1)$ resonant state, and (iii) transfers of energy from the $\text{Kr}(^3\Sigma_u^+)$ molecular states to the $\text{Xe}(^3P_1)$ resonant level in two-body collisions with Xe ground-state atoms. We now discuss each of these processes in more detail.

The quenching rate $k_q(1165 \text{ \AA}) = 1.2 \times 10^5 \text{ sec}^{-1}/\text{Torr}$ for the $\text{Kr}(^1P_1)$ resonant state is assumed to represent two-body collisional energy transfers to $\text{Xe}(7s)$ levels. At room temperature (about 300 K) both $\text{Xe}(7s)$ levels lie within $3k_B T$ of the $\text{Kr}(^1P_1)$ level, and it is not possible to decide which $7s$ level is coupled to the $\text{Kr}(^1P_1)$ resonant state.

As stated earlier, the time dependence of the $\text{Kr}(^1P_1)$ population can be fit to a single-exponential decay curve. This implies that the $\text{Kr}(^1P_1)$ population is not significantly dependent on the population of other excited states of Kr or Xe. We, therefore, neglect any feedback mechanisms from Xe to $\text{Kr}(^1P_1)$ levels.

The quenching rate $k_q(1236 \text{ \AA}) = 9.5 \times 10^5 \text{ sec}^{-1}/\text{Torr}$ for the $\text{Kr}(^3P_1)$ resonant state is assumed to represent collisional transfers to either $\text{Xe}(5d)$ or $\text{Xe}(6p)$ levels. Figure 1 indicates that many of these states could be the possible acceptor of this energy.

At low Xe-impurity concentrations (less than 1%) the time dependence of the $\text{Kr}(^3P_1)$ population could be predicted by a single-exponential decay. However, at larger impurity concentrations a second low-amplitude decay was seen. Intensity limitations prevented us from obtaining a systematic pressure dependence for this slow component. Nevertheless, this second component indicates that the $\text{Kr}(^3P_1)$ population is dependent on the population of other Kr or Xe excited species. The fact that this emission was seen at larger Xe-impurity concentrations implies that the coupling of $\text{Kr}(^3P_1)$ is with an excited state of Xe, most likely $\text{Xe}(5d)$ or $\text{Xe}(6p)$. We, therefore, believe there is a noticeable feedback mechanism from excited states of Xe to the $\text{Kr}(^3P_1)$ resonant level. Time-dependent measurements made in the Kr_2^* first continuum showed an identical effect.

After energy is transferred to excited states of Xe, radiative cascading in the $5d$ or $6p$ levels could populate the lower-lying states of Xe. Figures 1 and 3 suggest that radiative cascading in Xe eventually transfers energy from $\text{Kr}(^3P_1)$ levels to $\text{Xe}(^3P_1)$ levels. Grosf and Targ¹³ have shown that radiative cascading in Xe is enhanced in Kr-

Xe mixtures further supporting this view.

Figure 4 shows an absorption band in the Kr_2^* first continuum. This absorption band is centered at about 1296 \AA , the resonant wavelength of the $\text{Xe}(^1P_1)$ state. Like Castex¹⁴ and Freeman and Yoshina,¹⁵ we attribute this absorption to the $\text{Xe}(^1P_1)$ state. Other excited Xe levels in this region are dismissed as possible candidates because they do not have allowed transitions to the $\text{Xe}(^1S_0)$ ground state. We propose that molecular radiation in the Kr_2^* first continuum that coincides with the resonant wavelength of the $\text{Xe}(^1P_1)$ state is absorbed by $\text{Xe}(^1S_0)$ ground-state atoms creating a population of $\text{Xe}(^1P_1)$ excited states.

Time-dependent measurements taken in the vicinity of the absorption well indicate that the absorption process is rate limited by the decay of the $\text{Kr}(^3P_1)$ resonant state. Table I clearly shows that, with the exception of the resonant-trapped term associated with the $\text{Kr}(^3P_1)$ state, the pressure-dependent lifetimes of the $\text{Kr}(^3P_1)$ resonant state and the Kr_2^* first continuum are identical. This is expected because the Kr_2^* first continuum is commonly attributed to transitions from $\text{Kr}_2^*(0_u^+)$ molecular states (Hund's case *a*) to the repulsive ground state or from vibrationally relaxed $\text{Kr}_2^*(^1\Sigma_u^+)$ molecular states (Hund's case *c*) to the ground state.¹⁶ We cannot distinguish between these two emissions except to note that at longer wavelengths the emissions should be from $\text{Kr}_2^*(^1\Sigma_u^+)$. A thorough discussion of these molecular levels can be found in Ref. 17. Both Mulliken¹⁶ and Barr *et al.*¹⁷ associate the $\text{Kr}(^3P_1)$ with the Kr_2^* first continuum. Our time-dependent results support this assignment as does the work of Leichner and Ericson.²

No evidence of collisional energy transfers between $\text{Kr}_2^*(0_u^+)$ and Xe ground-state atoms was found. This was expected considering the short radiative lifetime of the molecular levels [about 5 nsec (Ref. 18)] that radiate in the 1290-\AA region. The short radiative lifetime associated with the $\text{Kr}_2^*(0_u^+)$ molecular state means that nonradiative energy transfers between $\text{Kr}_2^*(0_u^+)$ molecular states and Xe need not be considered.¹⁰ The time-independent emission spectra that we have presented in Figs. 3–5 show that the quenching of the Kr_2^* first continuum by collisional processes is much less than the quenching processes in the Kr_2^* second continuum where the cross sections for nonradiative energy transfers to Xe are much larger as we discuss later. A useful comparison can be made to the Ar-Xe (Refs. 11 and 19) system where the radiation from the long-lived $\text{Ar}_2^*(^3\Sigma_u^+)$ molecular state overlaps the resonant wavelength of the $\text{Xe}(^1P_1)$ resonant state and collisional transfers to $\text{Xe}(^1P_1)$ are very efficient. In those studies and in preliminary investigations of Ar-Xe in this laboratory, collisional processes effectively quench the molecular emissions in the 1290-\AA region. However, in Kr-Xe the emission spectra in the 1290-\AA region are not characteristic of the flat, rapidly quenched spectra associated with collisional quenching.

An interesting problem posed by this investigation is that the $\text{Xe}(^1P_1)$ resonant state appears not to radiate to the $\text{Xe}(^1S_0)$ ground state. In studies of pure Xe (Ref. 4) the absence of emissions at 1296 \AA has also been noted. Cheshnovsky *et al.*¹¹ have speculated that the $\text{Xe}(^1P_1)$

population may be collisionally depleted by transferring energy to the lower-lying Xe($6p$) level, Xe(3D_1). They then suggest that the Xe(3D_1) is linked to the Xe(3P_1) resonant state and the Xe(3P_2) metastable by radiative cascading in Xe. We note that this mechanism could provide an energetic link between Kr $_2^*(0_u^+)$ molecules and the Xe(3P_1) resonant state.

Again comparison to Ar-Xe has shown that the Xe(1P_1) state does emit resonant radiation at 1296 Å in that system. This means that the population of Xe(1P_1) in the Ar-Xe system is large enough so that the energy-transfer mechanism that depletes the Xe(1P_1) population does not completely quench the Xe(1P_1) population as it appears to do in pure Xe and in Kr-Xe mixtures. This comparison demonstrates that the absorption mechanism that we have identified in Kr-Xe mixtures is fairly inefficient when compared to collisional processes that populate the Xe(1P_1) resonant state in Ar-Xe.

It is interesting to note the different molecular mechanisms that populate the Xe(1P_1) state and the Xe(3P_1) state in Kr-Xe mixtures. As noted, the Xe(1P_1) resonant state seems to be populated by radiation from the short-lived Kr $_2^*(0_u^+)$ state, but the Xe(3P_1) level lies in the wavelength region of the long-lived Kr $_2^*(^3\Sigma_u^+)$ molecular state. This state has a radiative lifetime of about 250 nsec.²⁰ As with the Xe(1P_1) in Ar-Xe mixtures, we expect binary collisions to play an important role in transferring energy from $^3\Sigma_u^+$ molecular states to Xe excited states. Working at Xe impurity concentrations of about 0.1% or less, Salamero *et al.*⁸ have reported a binary rate of about $2 \times 10^7 P_{Xe} \text{ sec}^{-1}$ for the quenching of Kr $_2^*(^3\Sigma_u^+)$ by Xe(1S_0). This large rate is in agreement with the theoretical work of Gedanken *et al.*¹⁰ who predict large cross sections for energy transfers from $^3\Sigma_u^+$ molecular states to atomic resonant states if the energy level of the resonant state lies in the radiative continuum of the molecular emissions. Theoretical predictions^{8,10} yield a rate of about $10^7 P_{Xe} \text{ sec}^{-1}$ for transfers between Kr $_2^*(^3\Sigma_u^+)$ and Xe(3P_1).

Table I gives the pressure dependence that we have measured for emissions in the 1430-Å region. Within experimental error these emissions have the same pressure dependence that was found in the Kr $_2^*$ first continuum. These measurements may represent transitions from either $^1\Sigma_u^+$ or $^3\Sigma_u^+$ molecular states to the repulsive ground state.¹⁶ Within our pressure range we are unable to determine which would be the appropriate assignment. Of particular significance here is the fact that this is the first time-dependent study that directly links the Kr(3P_1) resonant state to emissions in the Kr $_2^*$ second continuum. We discuss this more fully in a work that presents a detailed model of excimer formation and decay in pure Kr.

Our time-dependent spectra shown in Figs. 4 and 5 qualitatively illustrate the efficiency of the molecule-atom energy transfer between Kr $_2^*(^3\Sigma_u^+)$ and Xe(3P_1). Unfortunately, we can make no definitive statements from our time-dependent results obtained at 1430 Å other than to present the results as we have done for the use of other researchers who may have use for these measurements. However, it is important to note that if the emissions that we have monitored in the Kr $_2^*$ second continuum

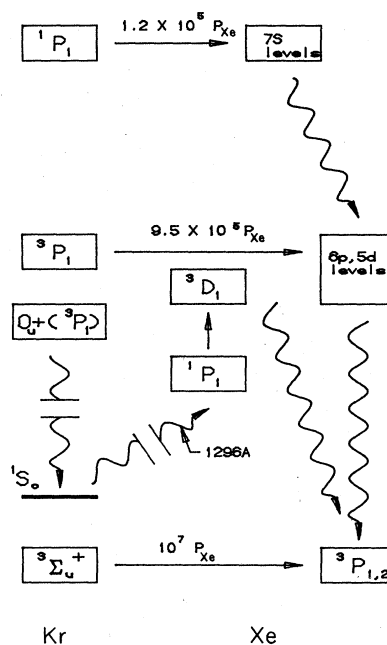


FIG. 14. Block diagram showing our model of energy transfers from Kr to Xe.

represent radiation from the Kr $_2^*(^3\Sigma_u^+)$ molecular state, then the binary energy transfer between Kr $_2^*(^3\Sigma_u^+)$ and Xe(3P_1) is rate limited by the Kr(3P_1) resonant state in our pressure range.

Finally, a proposed model for collisional and radiative energy transfers from Kr to Xe is presented in Fig. 14. This model illustrates only the measurements that we have obtained in this work. There are other reports that indicate that energy is transferred efficiently from the Kr(3P_2) metastable to Xe($5d, 6p$) levels⁹ and that, at higher pressures, the Xe(3P_1) resonant state absorbs radiation in the Kr $_2^*$ second-continuum region.¹⁴

Our time-independent spectra indicate that the energy transferred from Kr to Xe eventually populates the Xe($^3P_{1,2}$) excited states. Our model proposes that radiative cascading in Xe links the Xe(3P_1) resonant state with higher-lying excited states of Xe.

SUMMARY AND DISCUSSION

It has been found that the Kr(1P_1) and Kr(3P_1) resonance levels are rapidly quenched in two-body collisions with Xe ground-state atoms at the rates $1.2 \times 10^5 P_{Xe}$ and $9.5 \times 10^5 P_{Xe}$ in units of sec^{-1} , respectively. These rates greatly exceed the self-quenching of the resonance states in pure Kr. The large quenching rates by Xe ground-state atoms were explained in terms of energy resonances which exist in the Kr-Xe system. Because of these resonances electronic energy can be rapidly transferred from the Kr resonance states to Xe excited atomic levels.

The measurements in the vuv have also shown that molecule-atom energy transfers play a significant role in populating the Xe(3P_1) level. Two types of transfer

mechanisms were observed. The first of these corresponds to absorption of Kr_2^* first-continuum emissions by ground-state Xe to form $\text{Xe}(^1P_1)$ atoms. It was proposed that the population of the $\text{Xe}(^1P_1)$ resonance state is subsequently converted to $\text{Xe}(^3P_1)$ and $\text{Xe}(^3P_2)$ via the $\text{Xe}(^3D_1)$ level. This process was first suggested by Cheshnovsky *et al.*¹¹ on the basis of a time-unresolved study. A second energy-transfer mechanism involves direct excitation of the $\text{Xe}(^3P_1)$ level in two-body collisions with the long-lived $\text{Kr}_2^*(^3\Sigma_u^+)$ molecules. The experimental data indicate that this is essentially an energy resonance process in which the long-lived excimer is destroyed as rapidly as it is produced.

In conclusion, we have found that energy is transferred efficiently from Kr to Xe by a number of different chan-

nels. Further study of the Kr-Xe system is needed to completely determine the possible quenching mechanisms in Kr. In particular, a direct measurement of the pressure-dependent lifetime of the $\text{Kr}(^3P_0)$ metastable is required to present a complete picture of the quenching of Kr by Xe. Additional study of Kr-Xe at higher Kr pressures and smaller Xe impurity concentrations could yield valuable information about the formation processes that produce the molecular states that radiate in the Kr_2^* second continuum.

ACKNOWLEDGMENTS

This work was supported in part by USERDA through Oak Ridge National Laboratory.

*Present address: Johns Hopkins Hospital, Department of Radiation Oncology, 600 North Wolfe Street, Baltimore, Maryland 21205.

¹N. Thonnard and G. S. Hurst, *Phys. Rev. A* **5**, 1110 (1972).

²P. K. Leichner and R. J. Ericson, *Phys. Rev. A* **9**, 251 (1974).

³P. K. Leichner, *Phys. Rev. A* **8**, 815 (1973).

⁴P. K. Leichner, K. F. Palmer, J. D. Cook, and M. Thieneman, *Phys. Rev. A* **13**, 1787 (1976).

⁵P. K. Leichner, J. D. Cook, and S. J. Luerman, *Phys. Rev. A* **12**, 2501 (1975).

⁶C. K. Rhodes, *IEEE J. Quant. Electron.* **QE-10**, 153 (1974).

⁷C. E. Moore, *Atomic Energy Levels*, Natl. Bur. Stand. (U.S.) Circ. No. 467 (U.S. GPO, Washington, D.C., 1949), Vol. 2, p. 169, and Vol. 3, p. 114.

⁸Y. Salamero, A. Birot, H. Burnet, H. Dijols, J. Galy, P. Millet, and J. P. Montagne, *J. Chem. Phys.* **74**, 288 (1981).

⁹J. E. Velazco, J. H. Kolts, and D. W. Setser, *J. Chem. Phys.* **69**, 4357 (1978).

¹⁰A. Gedanken, J. Jortner, B. Raz, and A. Szoke, *J. Chem. Phys.* **57**, 3456 (1972).

¹¹O. Cheshnovsky, B. Raz, and J. Jortner, *J. Chem. Phys.* **59**, 3301 (1973).

¹²M. Thieneman, Ph.D. Thesis, University of Kentucky, 1977 (unpublished).

¹³G. Grosf and R. Targ, *Appl. Opt.* **2**, 299 (1963).

¹⁴M. C. Castex, *J. Chem. Phys.* **66**, 3853 (1977).

¹⁵D. E. Freeman and K. Yoshino, *J. Chem. Phys.* **67**, 3462 (1977).

¹⁶R. S. Mulliken, *Radiat. Res.* **59**, 357 (1974).

¹⁷T. L. Barr, D. Dee, and F. T. Gilmore, *J. Quant. Spectrosc. Radiat. Transfer* **15**, 625 (1975).

¹⁸No exact values exist for this state. Best estimates are usually given as the radiative lifetime associated with the $\text{Kr}(^3P_1)$ resonant state or by using values of similar states of Xe.

¹⁹H. Brunet, A. Birot, H. Dijols, J. Galy, P. Millet, and J. Salamero, *J. Phys. B* **15**, 2945 (1982).

²⁰Y. Salamero, A. Birot, H. Brunet, J. Galy, and J. P. Montagne, *J. Phys. B* **12**, 419 (1978).

²¹R. Turner, *Phys. Rev.* **158**, 121 (1967).